© 2017. Published by The Company of Biologists Ltd | Development (2017) 144, 2982-2993 doi:10.1242/dev.149955

RESEARCH ARTICLE

Bmp signaling maintains a mesoderm progenitor cell state in the mouse tailbud

Richa Sharma[1], Maxwell E. R. Shafer[1], Eric Bareke[2], Mathieu Tremblay[1], Jacek Majewski[2] and Maxime Bouchard[1,*]

ABSTRACT

Caudal somites are generated from a pool of progenitor cells located in the tailbud region. These progenitor cells form the presomitic mesoderm that gradually differentiates into somites under the action of the segmentation clock. The signals responsible for tailbud mesoderm progenitor pool maintenance during axial elongation are still elusive. Here, we show that Bmp signaling is sufficient to activate the entire mesoderm progenitor gene signature in primary cultures of caudal mesoderm cells. Bmp signaling acts through the key regulatory genes brachyury (*T*) and *Nkx1-2* and contributes to the activation of several other regulators of the mesoderm progenitor gene network. In the absence of Bmp signaling, tailbud mesoderm progenitor cells acquire aberrant gene expression signatures of the heart, blood, muscle and skeletal embryonic lineages. Treatment of embryos with the Bmp inhibitor noggin confirmed the requirement for Bmp signaling for normal *T* expression and the prevention of abnormal lineage marker activation. Together, these results identify Bmp signaling as a non-cell-autonomous signal necessary for mesoderm progenitor cell homeostasis.

KEY WORDS: Bmp signaling, Fgf signaling, Mesoderm progenitor differentiation, Presomitic mesoderm, Mouse embryo patterning

INTRODUCTION

During gastrulation, cells from the epiblast migrate through the primitive streak and undergo epithelial-mesenchymal transition to form the mesodermal and endodermal layers. As the primitive streak regresses toward the caudal region of the embryo, mesoderm progenitors successively contribute to notochord, paraxial mesoderm (muscles and bones), intermediate mesoderm (urogenital system) and lateral plate mesoderm (heart, gut and vasculature). Towards the end of gastrulation, somitogenesis proceeds from a pool of mesoderm tailbud progenitors responsible for generating caudal somites and tail elongation (Bénazéraf et al., 2010; Neijts et al., 2014; Wilson et al., 2009). Mesoderm progenitor cells form the presomitic mesoderm (PSM), which is progressively segmented into metameric units under the control of the segmentation clock (reviewed by Hubaud and Pourquié, 2014). The molecular network governing the transition from mesoderm progenitors to somites is well documented (Neijts et al., 2014; Wilson et al., 2009). In mouse and chick embryos, this network involves a signaling core that includes Wnt3a, brachyury (T) and Fgf8, which regulate downstream effectors of the segmentation clock (Galceran et al., 2001; Yamaguchi et al., 1999) and prevent retinoic acid-mediated differentiation of mesoderm cells (Diez del Corral et al., 2003). In this system, Fgf signaling is thought to maintain PSM cells in a progenitor state by activation of the retinoic acid-inactivating enzyme Cyp26a1 (Diez del Corral et al., 2003; Wahl et al., 2007). As mesoderm cells exit the Fgf8 gradient in the PSM, an increase in retinoic acid promotes their differentiation (Diez del Corral et al., 2003). Fgf signaling further regulates the migration of PSM cells toward the rostral region, where Fgf8 acts as a repellent signal from the caudal trunk/tailbud region, and Fgf4 acts as an attractive signal in the anterior streak and node region (Yang et al., 2002).

Bmp4, a member of the TGFβ superfamily, is also involved in somite formation. In frog and chick embryos, both gain- and loss-of-function studies identified a role for Bmp4 and Bmpr1 in tailbud outgrowth and somite differentiation (Beck et al., 2001; Reshef et al., 1998; Row and Kimelman, 2009). In zebrafish, loss of Bmp results in ventral fin and tail mesoderm defects (Pyati et al., 2005; Stickney et al., 2007). However, similar comprehensive studies on the later role of Bmp signaling in axis elongation and tail somite formation in mice have been hampered by the essential role of Bmp4 during gastrulation (Winnier et al., 1995). The few *Bmp4*-deficient embryos reaching a later stage show an axis elongation defect, which supports a role in posterior trunk elongation and patterning (Winnier et al., 1995). Accordingly, inactivation of noggin, an inhibitor of Bmp4 in this system (Wijgerde et al., 2005), leads to defects in elongation and in somite differentiation (McMahon et al., 1998; Wijgerde et al., 2005). However, the role of Bmp signaling in tailbud mesoderm progenitors remains poorly understood at the cellular and molecular levels.

To better understand the regulation of mesoderm progenitor differentiation we took advantage of a BAC transgenic line expressing GFP under the control of the *Pax2* locus. Although *Pax2* gene inactivation does not affect somitogenesis or axial elongation, the *Pax2* locus is specifically expressed in a graded fashion in the caudal region of the embryo (Bouchard et al., 2005, 2002; Kuschert et al., 2001). Using this transgene to isolate a population of tailbud mesoderm progenitor cells, we identified a crucial role for Bmp signaling in sustaining the entire network of mesoderm progenitor cells and preventing their premature differentiation into mesoderm derivatives such as muscle, cartilage, heart, vasculature and blood cells.

RESULTS

Maintenance of reporter gene expression in tailbud mesoderm progenitor cells requires a paracrine signal

To better understand the maintenance of progenitor cell identity in the tailbud, we used the *Pax2-GFP* BAC transgenic line, which

[1]Goodman Cancer Research Centre and Department of Biochemistry, McGill University, Montreal, Canada H3A 1A3. [2]Department of Human Genetics, McGill University and Genome Quebec Innovation Centre, Montreal, Canada H3A 0G1.

*Author for correspondence (maxime.bouchard@mcgill.ca)

M.B., 0000-0002-7619-9680

Received 1 February 2017; Accepted 10 July 2017

Development (2017) 144, 2982-2993 doi:10.1242/dev.149955

accurately expresses GFP in Pax2-expressing cells (Bouchard et al., 2005), including the nephric duct, tailbud, PSM and ventral mesoderm (Fig. 1A,B). We used fluorescence-activated cell sorting (FACS) to isolate GFP^{+} cells from the tailbud and cultured them on growth-arrested mouse embryonic fibroblasts (MEFs), which promotes their long-term survival (Fig. 1C,D). Interestingly, the vast majority of Pax2-GFP-expressing cells gradually lost their fluorescent signal over a period of 96 h, without significant cell death (Fig. 1E,F, Fig. S1A). We hereby refer to cells expressing the *Pax2-GFP* BAC transgene as Pax2-GFP^{on} and cells that downregulate GFP expression in primary cultures as Pax2-GFP^{off}. qRT-PCR analysis of cultured Pax2-GFP^{off} cells (separated from PKH26-labeled MEFs by FACS) showed a marked reduction in the expression of tailbud mesoderm markers *T* and *Msgn1*, suggesting that a signal was required to maintain the mesoderm progenitor cell fate in 2D culture (Fig. 1G). The few remaining Pax2-GFP^{on} cells in 96 h cultures expressed the renal lineage markers *Pax8* and *Gata3*, indicating that a small number of renal cells were present in primary cell cultures but that the levels of Pax2-GFP were not significantly affected at 96 h in these cells (Fig. S1B).

To determine whether the tailbud progenitor cell fate was maintained by a secreted signal(s) from within this population, we plated Pax2-GFP^{on} cells in 3D Matrigel cultures at decreasing densities. These culture conditions allowed for the maintenance of Pax2-GFP expression when plated at high cell density (Fig. 1H). By contrast, Pax2-GFP^{on} mesoderm progenitor cells plated at lower

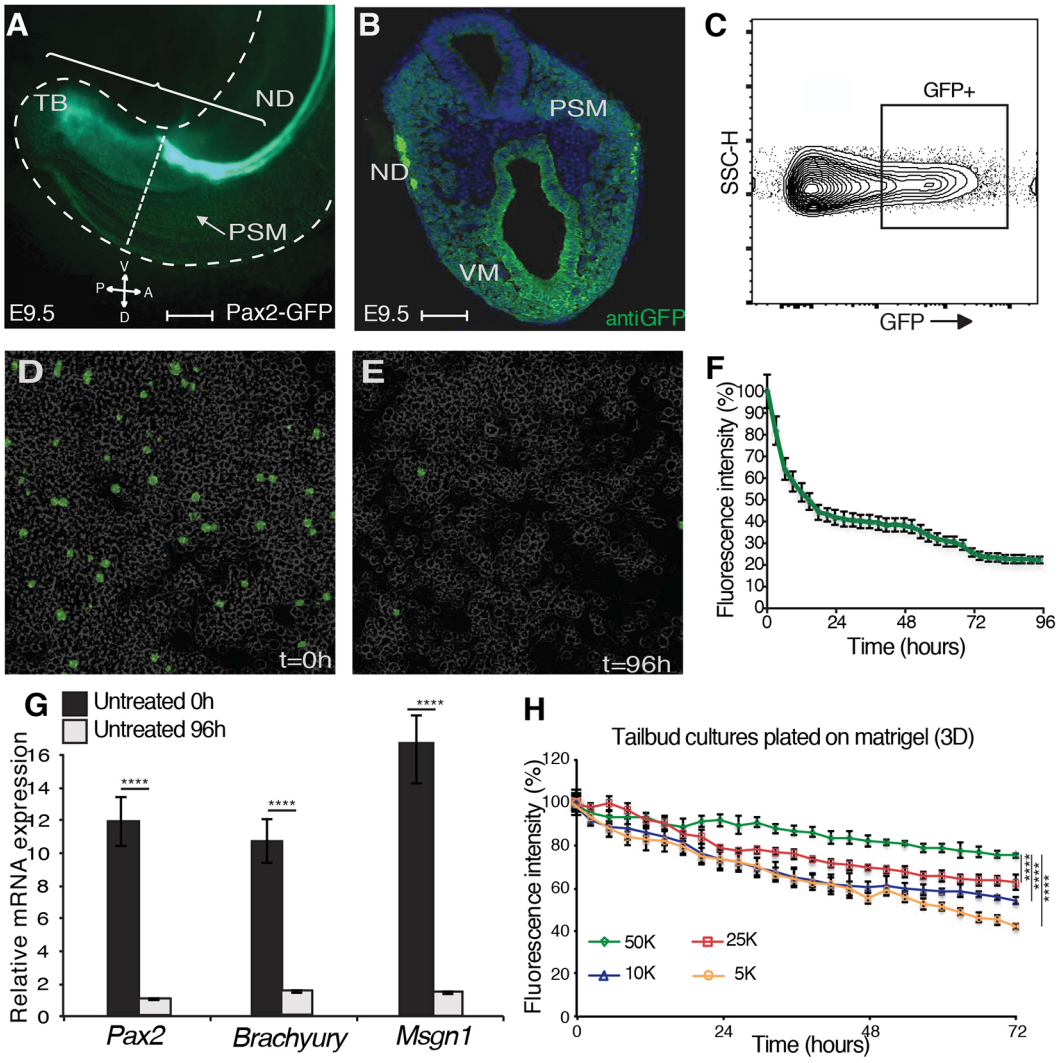

Fig. 1. Maintenance of *Pax2-GFP* reporter gene expression in the mesoderm progenitors of the tailbud requires the presence of a paracrine signal. (A) Endogenous fluorescence of *Pax2-GFP* BAC transgenic mice showing Pax2 expression in the tailbud (TB) and nephric duct (ND) of E9.5 embryos. The white dashed line across the tailbud in A indicates the approximate level of the transverse section shown in B. Bracket indicates region dissected for primary cultures. (B) Immunofluorescence against GFP in transverse section of *Pax2-GFP* BAC transgenic mice. PSM, presomitic mesoderm; VM, ventral mesoderm. Scale bars: 200 µm in A; 100 µm in B. (C) Representative FACS plot of tailbud cells from E9.5 embryos sorted based on Pax2-GFP expression. (D) Tailbud progenitor cells co-cultured with mitomycin C-treated MEFs showing initial expression levels of Pax2-GFP in all progenitors (note that MEFs are GFP^{-}). (E) Tailbud progenitor cells after 96 h of co-culture display a loss of Pax2-GFP fluorescence (original magnification 10×). (F) Quantification of Pax2-GFP expression over 96 h in culture. Shown is the fluorescence intensity (%) compared with *t*=0 h. (G) qRT-PCR of *Pax2*, brachyury (*T*) and *Msgn1* in *Pax2-GFP* tailbud mesoderm progenitors at 0 h and 96 h after co-culture. mRNA levels were normalized to *B2m* and Student's *t*-test was used to determine statistical differences. (H) Pax2-GFP^{+} tailbud mesoderm progenitor cells were plated at different densities in 3D Matrigel cultures and the average GFP fluorescence intensity was measured over 72 h with reference to the initial fluorescence levels (set at 100%). Statistical significance was calculated using one-way ANOVA analysis and all samples were compared with 50,000 (50K) cells, which maintain high GFP expression levels after 72 h in culture. (G,H) ****P<0.0001. Error bars indicate mean±s.d. n=6 embryos per experiment; three independent experiments.

Development (2017) 144, 2982-2993 doi:10.1242/dev.149955

densities led to a density-dependent decrease of Pax2-GFP signal, indicating that tailbud progenitor cell fate maintenance depends on the activity of a paracrine signal, which is likely to be diluted in 2D cultures (Fig. 1H).

Bmp4 is sufficient to restore mesoderm progenitor fate in Pax2-GFP^{off} cells

To identify the paracrine signal involved in mesoderm progenitor cell fate, we undertook a candidate approach. We initially tested the capacity of Wnt3a, Fgf8, Fgf4 and Bmp4 to reactivate GFP expression in Pax2-GFP^{off} cells (after 96 h in culture), all of which have previously been implicated in axis elongation (Wilson et al., 2009). Of these, only Bmp4 led to a strong GFP reactivation after 12 h of treatment, whereas the other factors were not sufficient to trigger a detectable response (Fig. 2A,B, Fig. S2A-C). This suggests that Bmp is an important paracrine factor for maintaining the tailbud progenitor fate. To validate this possibility, we treated progenitor cells plated at a high density in Matrigel (which maintain Pax2-GFP expression) with the Bmp inhibitor noggin. In contrast to untreated cells that maintain Pax2-GFP at high density in Matrigel (Fig. 1H), noggin treatment led to a significant decrease in Pax2-GFP expression, further supporting the importance for Bmp in this process (Fig. S2D-G). We determined the tailbud expression domain of *Bmp4* by *in situ* hybridization. *Bmp4* is expressed in the ventral but not in the dorsal mesoderm (Fig. S2H). Together, these results suggest that a ventral mesoderm source of Bmp acts on dorsal mesoderm progenitor cells.

Given the important roles of both Fgf4 and Fgf8 during trunk elongation, we assessed the response to Bmp4 in combination with these signaling molecules at different time points (Fig. 2A). Interestingly, the combination of Fgf8 and Bmp4 shortened the timing of GFP re-expression to 6 h, down from 12 h with Bmp4 alone (Fig. 2B,C). By contrast, addition of Fgf4 abrogated the response to Bmp4 (Fig. 2B,C). These experiments suggest that Fgf8 facilitates the response to Bmp signaling, whereas Fgf4 seems to counteract Bmp.

Bmp signaling maintains the entire mesoderm progenitor cell network

To gain further insight into the transcriptional control of mesoderm progenitor cell fate, we performed whole-transcriptome RNA sequencing (RNA-seq) on Pax2-GFP^{on} mesoderm progenitors (untreated at 0 h), Pax2-GFP^{off} cells (untreated at 96 h), and on mesoderm progenitor cells at 96 h treated with Bmp4 alone (5 h and 11 h post-treatment) or in combination with Fgf8 (5 h post-treatment) or Fgf4 (11 h post-treatment) (Fig. 2A, Fig. S3A,B, Tables S1-S12). Pairwise comparisons of these transcriptional profiles were performed to identify a gene signature associated with Pax2-GFP^{on} cells (Fig. S3A,B, Table S13). Gene ontology analysis of the Pax2-GFP^{on} gene signature (which contained 170 genes) showed a statistical enrichment for mesoderm lineage markers, specifically those of presomitic mesoderm and tailbud progenitor cells (Fig. 3A). In fact, most known mesoderm progenitor-associated genes were differentially regulated between Pax2-GFP^{on} (untreated at 0 h) and Pax2-GFP^{off} (untreated at 96 h), and were found to be expressed in all Pax2-GFP-expressing cells (Fig. 3B). Remarkably, these mesoderm markers, which included *Msgn1*, *T*, *Fgf8*, *Wnt5a*, *Wnt3a*, *Tbx6*, *Cdx2*, *Cdx4* and *Nkx1-2*, were also the most differentially regulated genes between untreated cells at 0 h and 96 h, and between Bmp4-treated (96+5 h) and untreated cells at 96 h (green dots, Fig. 3B,C,D, Table S15). These results indicate that the loss of Pax2-GFP expression is primarily associated with a loss of mesoderm progenitor cellular identity, and that Bmp4 alone is sufficient to re-establish the mesoderm progenitor gene signature (Fig. 3B-D, green dots). The Bmp4 response was supported by Fgf8 treatment, but was largely prevented by co-treatment with Fgf4 (Fig. 3B).

To confirm the RNA-seq results, we performed qRT-PCR analysis of key regulators of the mesoderm progenitor fate, which validated the loss of identity during the first 96 h in culture and the reactivation of these genes by Bmp4 (Fig. 3E). Hence, these results indicate that the maintenance of the mesoderm progenitor gene signature is largely dependent on the sustained activity of Bmp4, which can be modulated by Fgf signaling.

To better understand gene network activation by Bmp4, we performed qRT-PCR of key regulated genes in the presence of the translation inhibitor cycloheximide (CHX). This analysis identified three groups of mesoderm progenitor genes based on their response to Bmp4. Genes such as *T* and *Nkx1-2* were unaffected by the presence of CHX, indicating that they are direct targets of Bmp signaling (Fig. 4A). Others, such as *Msgn1* and *Cdx4*, were activated 3- to 4-fold in cells treated with Bmp4 plus CHX, but failed to reach the activation levels observed with Bmp4 alone (Fig. 4B). This suggests a direct regulation by Bmp signaling that is complemented by a Bmp-regulated coactivator. Finally, *Pax2* expression was found to be strictly dependent on translation, indicating that it is an indirect target of Bmp signaling activity (Fig. 4C).

From these results, we conclude that Bmp signaling is sufficient for the expression of several key regulators of mesoderm progenitor fate, resulting in the maintenance of the underlying gene regulatory network.

Bmp sustains the mesoderm progenitor cell lineage *in vivo*

To determine whether the maintenance of mesoderm progenitor cells by Bmp also occurs in the embryo, we treated *ex utero* mouse embryo cultures with the Bmp inhibitor noggin. *Pax2-GFP* embryos were dissected at E8.75 and maintained in rolling cultures for 36 h in the presence or absence of noggin. We observed a reduction of GFP signal intensity in noggin-treated versus control embryos (Fig. 5A-B′). We next visualized the effect of noggin by whole-mount *in situ* hybridization against *T*. In contrast to the high expression levels in control embryos, the addition of noggin to the culture medium resulted in a significant downregulation of *T* (Fig. 5C,D). The effect of Bmp inhibition was extended to the mesoderm progenitor markers *Nkx1-2*, *Msgn1* and *Pax2*, as shown by qRT-PCR of noggin-treated and control tailbud cells. These experiments confirmed that Bmp signaling is required to maintain the mesoderm progenitor transcriptional program *in vivo* (Fig. 5E).

Bmp signaling prevents aberrant differentiation of mesoderm progenitor cells

To identify the fate changes associated with the loss of mesoderm progenitor identity, we determined the gene signatures associated with Pax2-GFP^{off} cells using the pairwise comparisons performed previously (Fig. S3A,C, Table S14). Gene ontology analysis identified distinct signatures associated with muscle, heart, blood, bone and endothelial cell differentiation (Fig. 6A, Table S16). Genes associated with these ontological signatures were also among the most differentially regulated genes in Pax2-GFP^{off} (untreated at 96 h) compared with Pax2-GFP^{on} (untreated at 0 h) (colored dots, Fig. 6B). Treatment with Bmp4 alone or together with Fgf8 effectively downregulated these gene signatures, whereas Bmp4

Development (2017) 144, 2982-2993 doi:10.1242/dev.149955

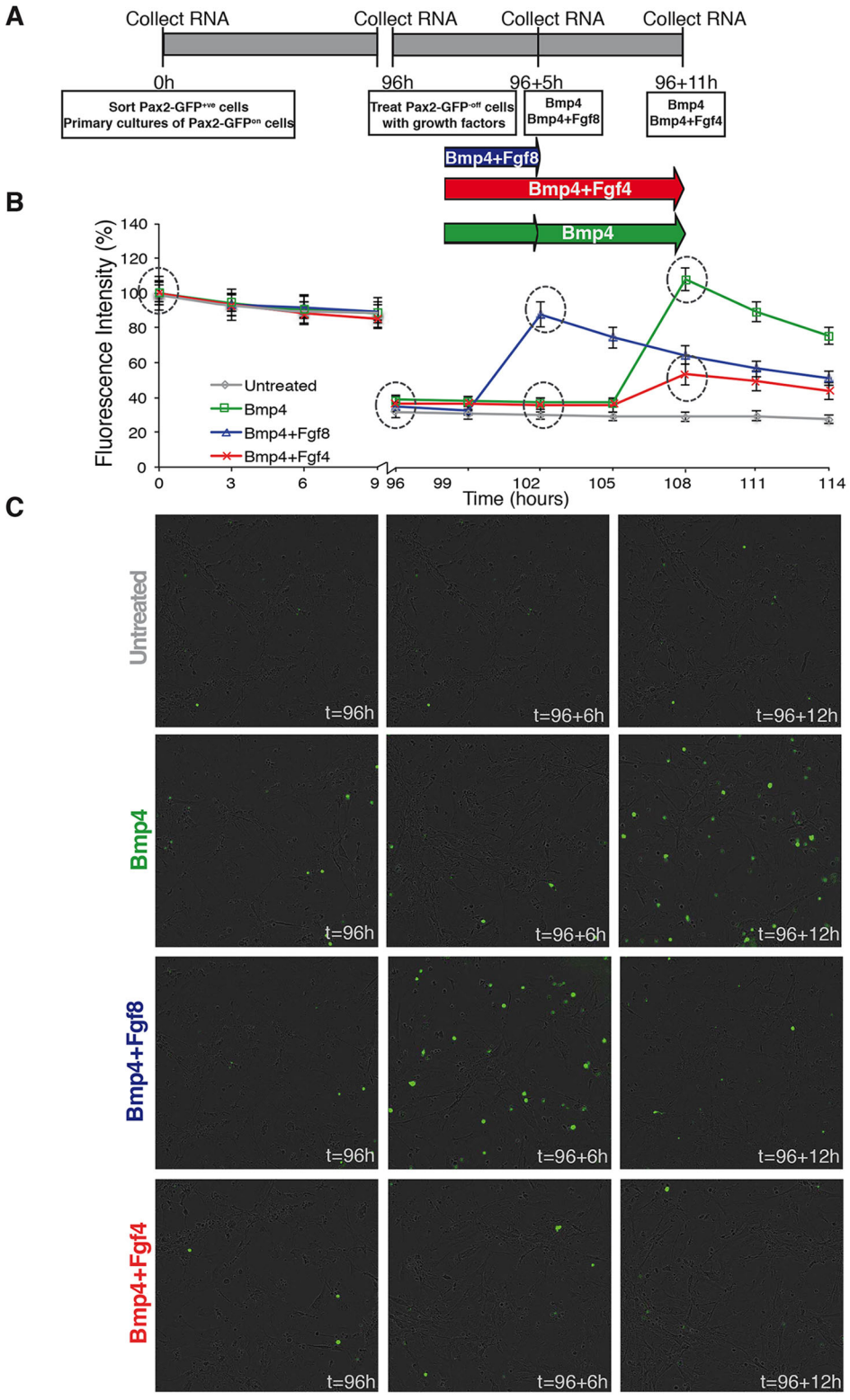

Fig. 2. Bmp4 is sufficient to reactivate Pax2-GFP expression in tailbud progenitors. (A) Timeline of *Pax2-GFP* BAC primary cell culture and treatments. (B) Measurement of Pax2-GFP fluorescence over 114 h in co-culture with MEFs. After 96 h the cultures are treated with Bmp4 in the presence or absence of Fgf4 or Fgf8. Circles indicate time points at which mRNA was collected for RNA-seq (untreated at 0 h, untreated at 96 h, Bmp4 at 96 +5 h, Bmp4+Fgf8 at 96+5 h, Bmp4 at 96+11 h and Bmp4+Fgf4 at 96+11 h). Average fluorescence intensity (%) was measured every 3 h with reference to *t*=0 h (set at 100%). Mean±s.d., *n*=6 embryos/experiment. (C) Representative images from the circled time points of Pax2-GFP^{+} tailbud progenitors in co-culture with MEFs untreated or treated with growth factors (original magnification 10×).

and Fgf4 generally failed to abrogate their expression (Fig. 6C, Table S16). The Bmp4 transcriptional response was validated by qRT-PCR analysis on a subset of differentially regulated genes (Fig. 6D). Here again, the Bmp4 response was supported by Fgf8, whereas Fgf4 negatively affected the regulation of a subset of Bmp-responsive genes (Fig. 6D).

To test whether Bmp activity affected the neural and hindgut tailbud cell fates, we tested markers for these lineages by qRT-PCR. We observed a response of *Sox2* and the hindgut markers *Sox17* and *Epha2* to Bmp4 in primary cultures but noggin treatment failed to validate a strong role for Bmp signaling in embryo cultures *ex utero* (Fig. S4A-D). Hence, Bmp signaling prevents the aberrant

Development (2017) 144, 2982-2993 doi:10.1242/dev.149955

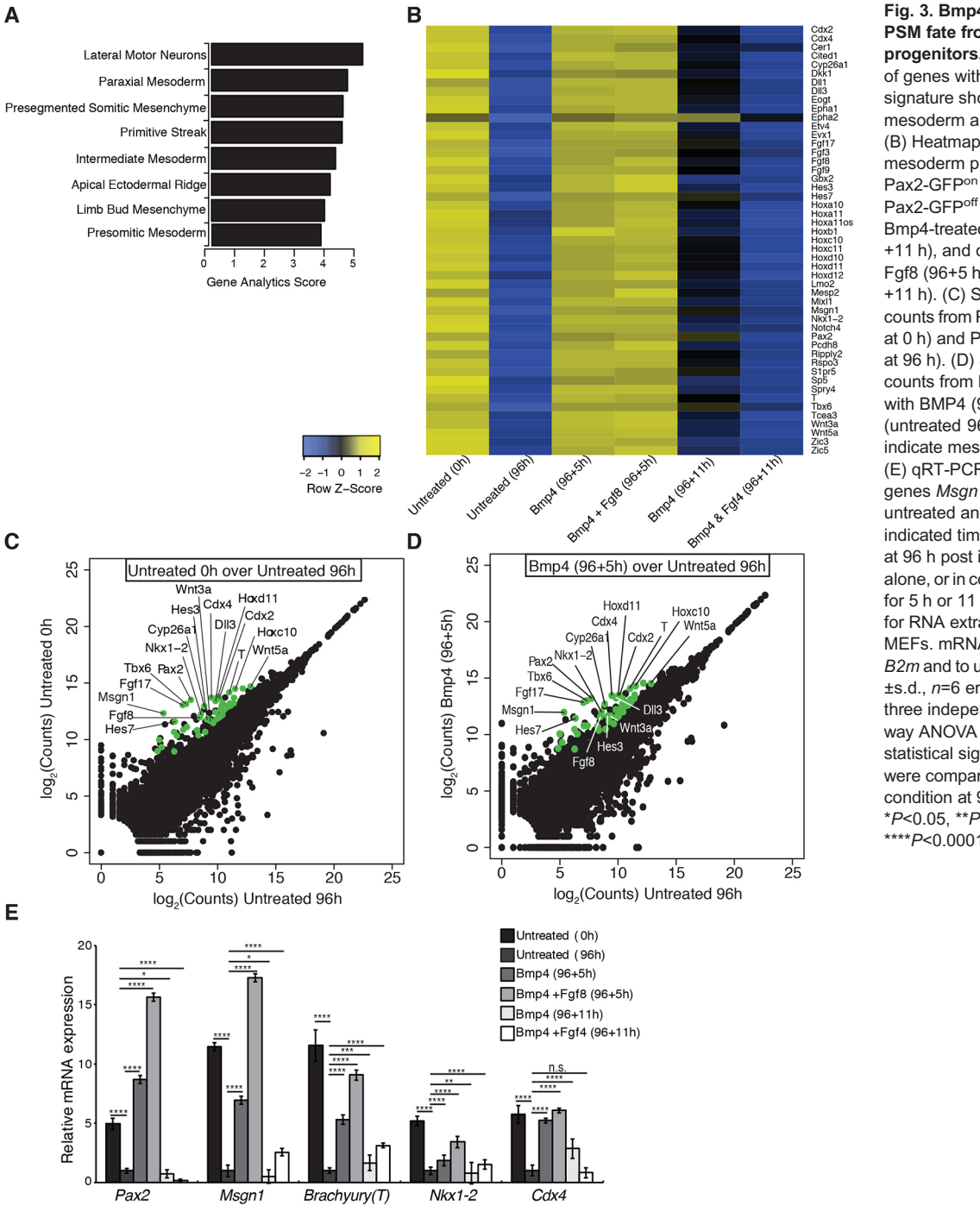

Fig. 3. Bmp4 is sufficient to induce PSM fate from Pax2-GFP^{off} tailbud progenitors. (A) Gene ontology analysis of genes within the Pax2-GFP^{on} gene signature showing enrichment for mesoderm and PSM markers. (B) Heatmap of mRNA read counts of mesoderm progenitor genes in Pax2-GFP^{on} cells (untreated at 0 h), Pax2-GFP^{off} cells (untreated at 96 h), Bmp4-treated cells (96+5 h and 96 +11 h), and cells treated with Bmp4 and Fgf8 (96+5 h) or Bmp4 and Fgf4 (96 +11 h). (C) Scatter plot of mRNA read counts from Pax2-GFP^{on} cells (untreated at 0 h) and Pax2-GFP^{off} cells (untreated at 96 h). (D) Scatter plot of RNA read counts from Pax2-GFP^{on} cells treated with BMP4 (96 h +5 h) and Pax2-GFP^{off} (untreated 96 h). Green dots (C,D) indicate mesoderm progenitor genes. (E) qRT-PCR of mesoderm progenitor genes *Msgn1*, *T*, *Nkx1-2* and *Cdx4* from untreated and treated cells at the indicated time points. Cells were treated at 96 h post initial plating with Bmp4 alone, or in combination with Fgf8 or Fgf4 for 5 h or 11 h, respectively. Cells used for RNA extraction were sorted out from MEFs. mRNA levels were normalized to *B2m* and to untreated cells at 96 h. Mean ±s.d., n=6 embryos per experiment; three independent experiments. One-way ANOVA was used to calculate statistical significance and all samples were compared with the untreated condition at 96 h. n.s., not significant; *P<0.05, **P<0.01, ***P<0.001, ****P<0.0001.

expression of cell differentiation markers primarily in tailbud mesodermal progenitor cells.

BMP signal inhibition upregulates aberrant lineage markers in whole embryos

We next tested if the transcriptional upregulation of differentiation markers within mesoderm progenitors upon loss of Bmp signaling led to a distinct commitment to these fates. Immunohistochemical analysis of cells at 0 h showed little expression of markers such as Ter119 (Ly76; blood), Pax7 (skeletal muscle) and Gata4 (heart) (Fig. 7A). However, the expression of these differentiation markers was upregulated after 96 h in culture (Fig. 7B). Strikingly, Pax2-GFP^{off} cells at 96 h frequently upregulated more than one lineage marker, indicating an aberrant and dysregulated differentiation process (Fig. 7B,D). This anomalous differentiation was lost when cells were treated with Bmp4 (Fig. 7C,D).

To test if the inhibition of Bmp signaling can cause aberrant differentiation of mesoderm progenitors in the developing embryo, we performed *ex utero* embryo cultures in the presence of noggin for 48 h. Noggin-treated embryos showed abnormalities in the development of the somites and neural tube, and a shortened caudal trunk (Fig. S4E,F). Immunohistochemical analysis of noggin-treated tailbud sections showed atypical morphology, with condensed cell clusters (Fig. 7F) and ectopic expression of Gata4 and Pax7. These abnormal structures contrasted with the morphology of control embryos (Fig. 7E). From these results we conclude that Bmp plays a

Development (2017) 144, 2982-2993 doi:10.1242/dev.149955

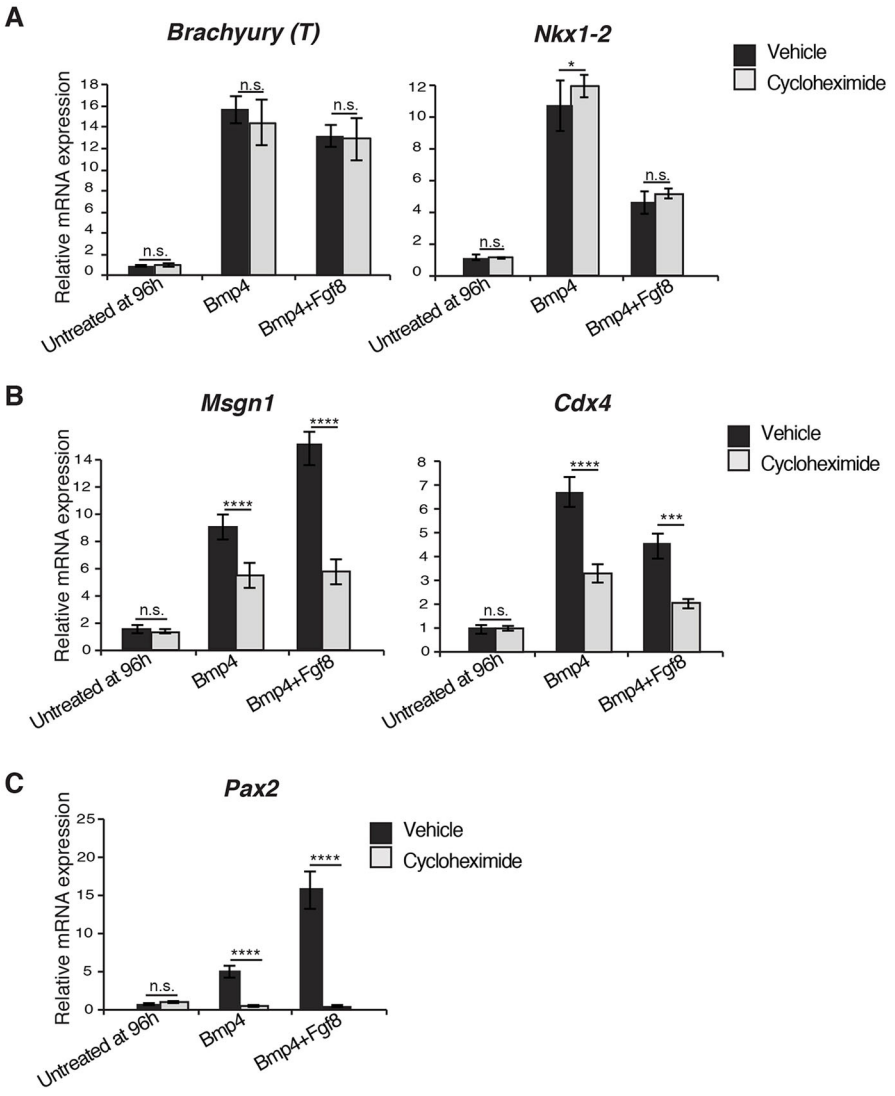

Fig. 4. Bmp4 is sufficient for maintenance of key regulators of the mesoderm progenitor cell fate. (A) qRT-PCR of *T* and *Nkx1-2* identifies translationally independent targets of Bmp4 in cells treated with Bmp4 alone (96+5 h) or Bmp4 and Fgf8 (96+5 h), grown in the presence or absence of cycloheximide (CHX). (B) qRT-PCR for *Msgn1* and *Cdx4* identifies genes partially affected by translation inhibition by CHX. (C) qRT-PCR for *Pax2* identifies an indirect Bmp target that strictly requires protein translation for activation. Cells were sorted out from MEFs and mRNA levels were normalized to *B2m* and all samples were compared with the vehicle-treated condition at 96 h. Student's *t*-test was used to determine statistical differences. Mean±s.d., $n=6$ embryos per experiment; three independent experiments. n.s., not significant; $^{*}P<0.05$, $^{***}P<0.001$, $^{****}P<0.0001$.

crucial role in maintaining mesoderm progenitors in an undifferentiated state, before commitment towards somitogenesis.

DISCUSSION

Axial elongation proceeds through the coordinated differentiation of progenitor cells to pattern the growing embryo. During this process, the formation of new somites is initiated in the caudal trunk region and involves the migration and differentiation of mesoderm progenitor cells. These progenitors upregulate somite differentiation markers as they exit the influence of caudal signals responsible for maintaining those cells in an undifferentiated state. In this report, we identified Bmp as a key signal responsible for mesoderm progenitor maintenance through the direct activation of several of the most important regulators of the mesoderm progenitor molecular network. We further identified a role for Bmp in preventing the aberrant activation of differentiation markers of mesoderm derivative tissues (muscle, heart, blood, bone and vasculature cell lineages). These experiments identify Bmp as a key regulator of mesoderm progenitor homeostasis in the tailbud.

Mesoderm progenitor maintenance

The process of somite formation from mesoderm progenitor cells has been studied extensively (Bénazéraf et al., 2010; Neijts et al., 2014; Wilson et al., 2009). The gene regulatory network underlying this process relies on complex signaling and transcriptional events. The apex of this network includes Wnt signaling (e.g. Wnt5a and Wnt3a), the transcription factor T and Fgf signaling (e.g. Fgf4 and Fgf8), which enter a mutual regulatory loop and regulate downstream patterning modules such as the establishment of the Notch-mediated segmentation clock, the repression of the retinoic acid differentiation signal and the activation of caudal Hox and Cdx patterning genes (Aulehla and Pourquie, 2010; Deschamps and van Nes, 2005; Hubaud and Pourquié, 2014; Wilson et al., 2009). In the mouse, very little is known about the role of Bmp signaling in mesoderm progenitor specification and maintenance (McMahon et al., 1998; Wijgerde et al., 2005). This is largely due to the crucial role of Bmp4 at an early stage of gastrulation (Winnier et al., 1995). In zebrafish, constitutive activation of the Bmp receptor Bmpr1b in the tailbud leads to an expansion of the T-positive mesoderm progenitor zone (Row and Kimelman, 2009), while transgenic expression of a dominant-negative version of the same receptor leads to ectopic tail formation (Pyati et al., 2005).

Here, we used a primary culture system to assess the role of signaling molecules in mesoderm progenitor maintenance in the mouse tailbud. Mesoderm progenitor cells in culture rapidly lose their identity and spontaneously upregulate aberrant cell

Development (2017) 144, 2982-2993 doi:10.1242/dev.149955

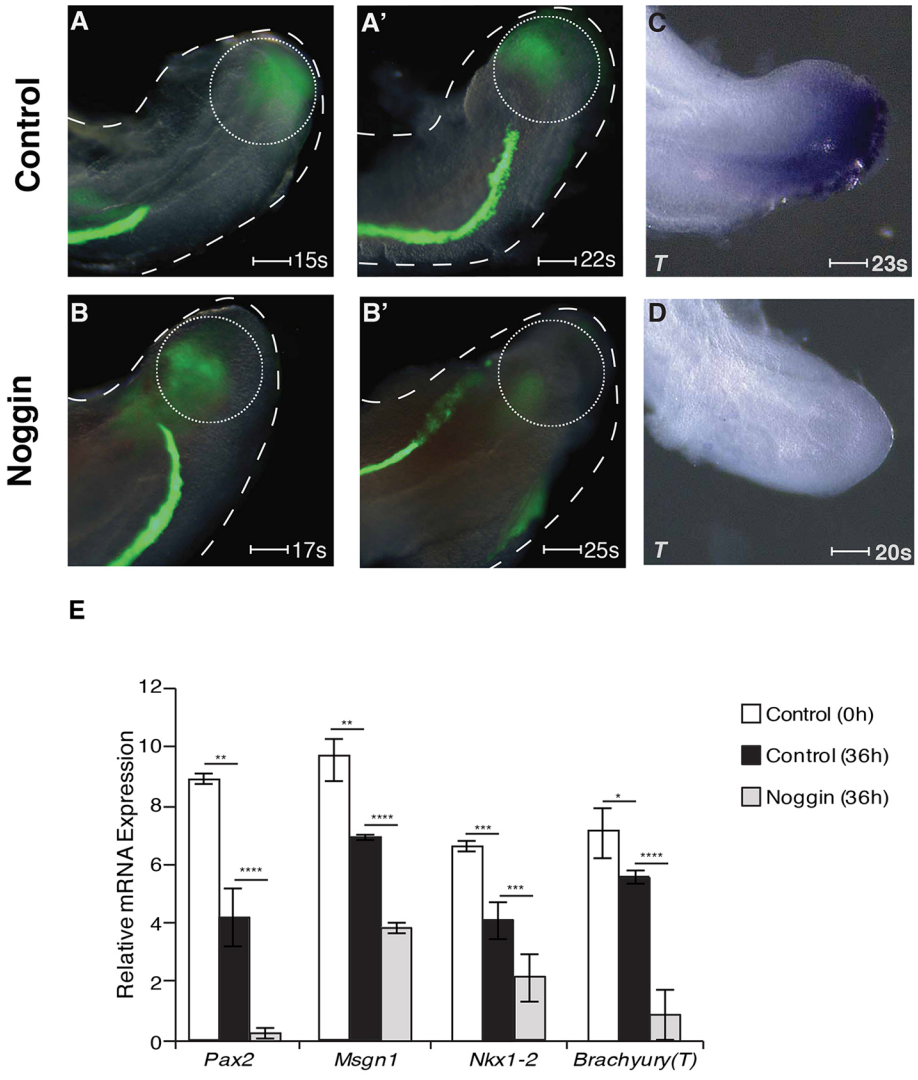

Fig. 5. Bmp4 in the tailbud sustains the PSM progenitor lineage *in vivo*. (A-B′) Pax2-GFP^{+} embryos dissected at E8.75 were cultured *ex utero* for 36 h in the presence (B,B′) or absence (A,A′) of noggin. Pax2-GFP expression in tailbud progenitors is circled. (C,D) Whole-mount *in situ* hybridization of the mesoderm progenitor marker *T* in embryos cultured in the absence (C) or presence (D) of noggin. s, somites. Scale bars: 200 µm. (E) qRT-PCR of mesoderm progenitor marker genes *Pax2*, *Msgn1*, *Nkx1-2* and *T* on tailbud of *ex utero* cultured embryos treated with and without noggin. Tailbud mRNA levels were normalized to *B2m*. One-way ANOVA was used to determine statistical differences and all samples were compared with control at 36 h. Mean±s.d., *n*=3 embryos per experiment; representative of four independent experiments. **P*<0.05, ***P*<0.01, ****P*<0.001, *****P*<0.0001.

differentiation markers. Supplementing with Bmp was sufficient to reactivate the entire mesoderm progenitor gene network within 5 h after treatment. This rapid response suggests that Bmp signaling regulates most genes in the network either directly or early in the transcriptional cascade. Specifically, we found that key network regulators such as *T*, *Nkx1-2*, *Msgn1* and *Cdx4* are either fully or partially responsive to Bmp signaling in the absence of protein translation, indicating a direct transcriptional response to Bmp signaling. Of interest, Bmp signaling and *T* have been found to genetically cooperate in tailbud progenitor cell differentiation (O'Neill and Thorpe, 2013). T was also reported to interact with the Bmp signaling molecule Smad1 (Messenger et al., 2005). Hence, the immediate response gene *T* might cooperate with Bmp-Smad signaling to promote the full mesoderm progenitor transcriptional response.

The capacity of Bmp4 to activate the mesoderm progenitor cell fate appears to act via a paracrine signaling mechanism. Plating mesoderm progenitor cells at high density in Matrigel maintained reporter gene expression in a Bmp-dependent manner, as shown by noggin treatment. The fact that this response was lost at lower density argues against an autocrine mechanism. Interestingly, Bmp4 is expressed in the ventral tailbud mesoderm, while most mesoderm progenitor regulatory genes are expressed in the more dorsal region (Inman and Downs, 2006; McMahon et al., 1998; Yoon et al., 2000). Together, these observations suggest a model by which ventral Bmp sustains a dorsal mesoderm progenitor cell fate. Pax2-GFP was expressed in both the ventral Bmp-expressing cells and the dorsal PSM progenitor cells, allowing us to observe the interaction between both compartments.

The fact that our analyses did not identify an overt neural or endodermal signature between Bmp-treated and untreated cells might reflect a more prominent role of Bmp in activating the mesoderm progenitor response. Alternatively, it might reflect the origin of the cells isolated on the basis of Pax2-GFP expression, or a differential maintenance of certain cell types in our culture conditions. In either case, the strong and widespread mesodermal response of *Pax2-GFP* cells to Bmp treatment unequivocally identifies an important role for this pathway in the maintenance of mesoderm progenitor cell fate.

Our data suggest that Fgf4 and Fgf8 have differential roles during mesoderm progenitor maintenance. Whereas Fgf8 had a positive effect on the global response to Bmp signaling, Fgf4 negatively affected this response for a large proportion of Bmp-responsive genes. Such opposing roles for Fgf4 and Fgf8 have been observed in mesoderm progenitor cell migration (Yang et al., 2002). The opposite roles of Fgf4 and Fgf8 in Bmp4 signaling and mesoderm progenitor migration contrast with the functional redundancy

Development (2017) 144, 2982-2993 doi:10.1242/dev.149955

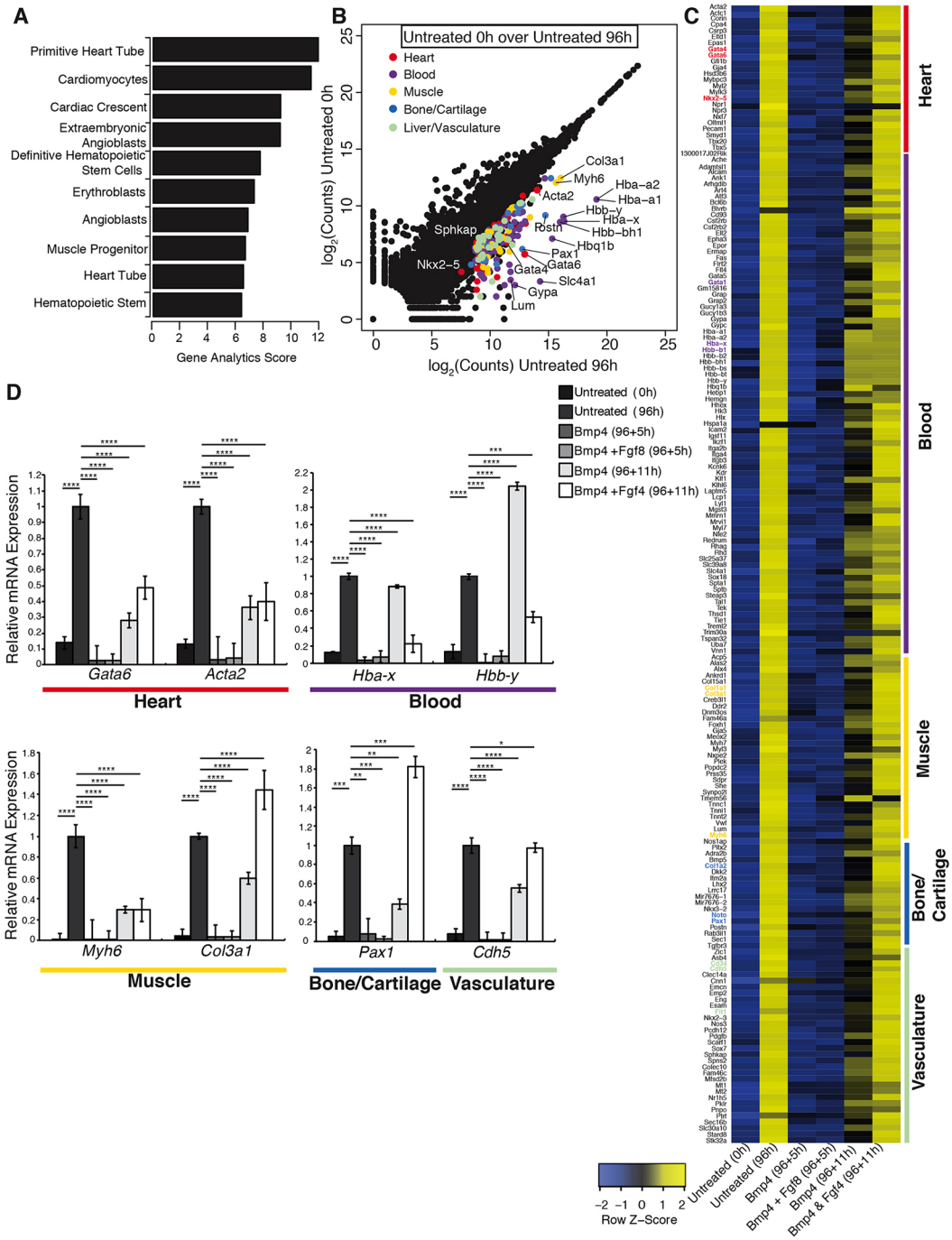

Fig. 6. Bmp4 signaling prevents aberrant differentiation of mesoderm progenitors. (A) Gene ontology analysis of genes within the Pax2-GFP^{off} profile showing enrichment for heart, blood, vasculature and muscle signatures. (B) Scatter plot of RNA read counts from Pax2-GFP^{on} cells (untreated at 0 h) and Pax2-GFP^{off} (untreated at 96 h). Colored dots indicated differentiated lineage marker genes. (C) Heatmap of RNA read counts of differentiated lineage marker genes in Pax2-GFP^{on} cells (untreated at 0 h), Pax2-GFP^{off} (untreated at 96 h), treated with Bmp4 (96+5 h and 96+11 h) and treated with Bmp4 plus Fgf8 (96+5 h) or Bmp4 plus Fgf4 (96+11 h). Canonical lineage markers are highlighted. (D) qRT-PCR of differentiated lineage markers from untreated and treated cells. Cells were treated with Bmp4 alone, or in combination with Fgf8 or Fgf4 at 96 h post initial plating for 5 h or 11 h, respectively. Cells used for RNA extraction were sorted out from MEFs. mRNA levels are normalized to *B2m* and to untreated cells at 96 h. Mean±s.d., *n*=6 embryos per experiment; three independent experiments. One-way ANOVA was used to calculate statistical significance and all samples were compared with untreated at 96 h. **P*<0.05, ***P*<0.01, ****P*<0.001, *****P*<0.0001.

observed in mesoderm patterning (Naiche et al., 2011; Boulet and Capecchi, 2012). Whereas single-knockout embryos form normal somites, *Fgf4;Fgf8* double-knockout embryos show important axial elongation and somitogenesis defects accompanied by premature differentiation of PSM cells toward the somitic fate (Naiche et al., 2011; Boulet and Capecchi, 2012). Hence, it is possible that Fgf4 has a dual function during mesodermal cell maturation. It might act redundantly with Fgf8 in the PSM region, and contribute to the termination of Bmp signaling in the more anterior paraxial mesoderm region. The expression of Fgf4 in the primitive streak region, anterior of Fgf8 expression (Welsh and O'Brien, 2000; Boulet and Capecchi, 2012), is compatible with this possibility.

Development (2017) 144, 2982-2993 doi:10.1242/dev.149955

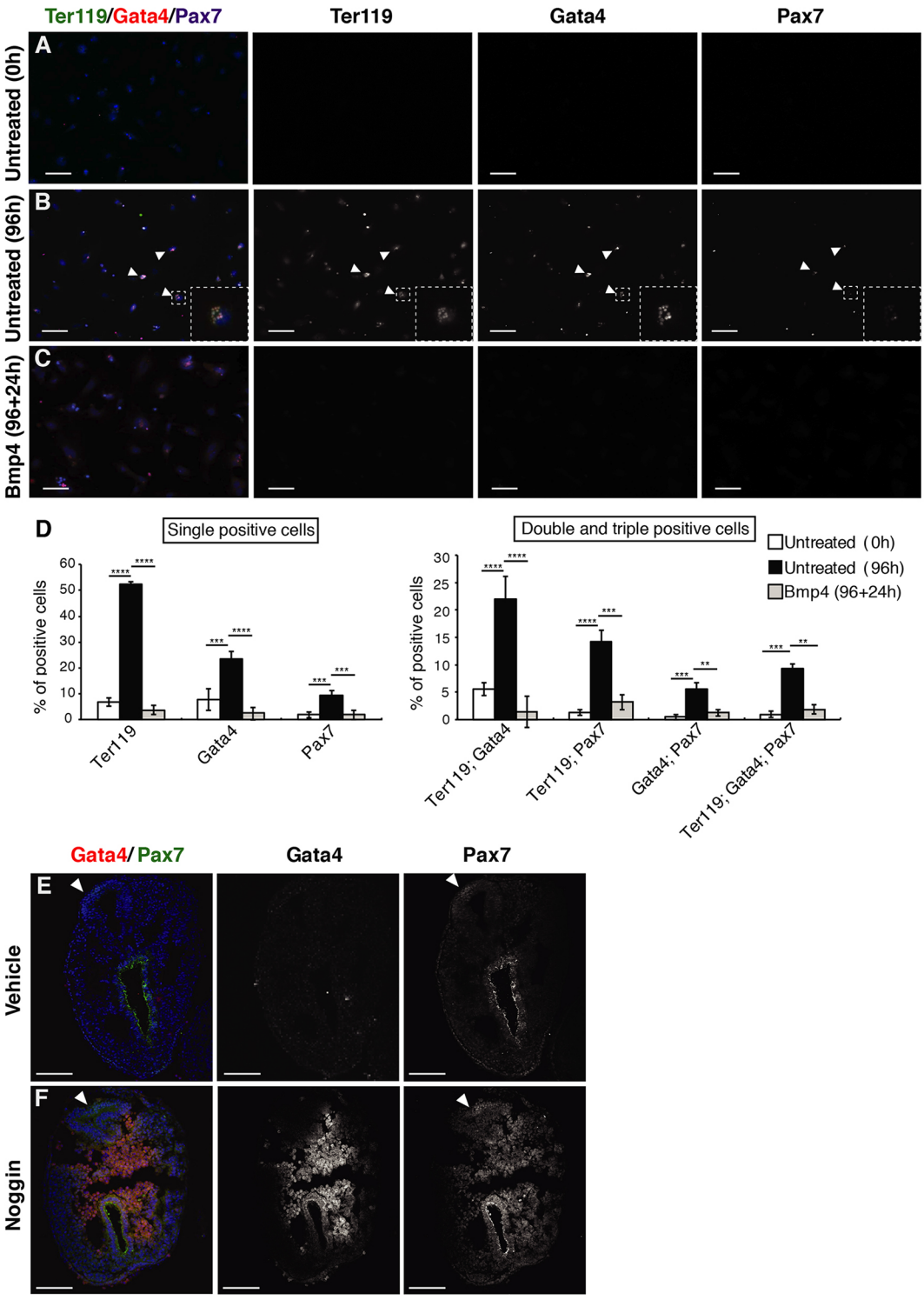

Fig. 7. Inhibition of Bmp4 signaling upregulates differentiation lineages *in vivo*. (A-C) Immunocytochemistry on mesoderm progenitor cells shows an upregulation of blood (Ter119), heart (Gata4) and skeletal muscle (Pax7) markers after 96 h of *in vitro* culture. This upregulation is lost when mesoderm progenitor cells were treated with recombinant Bmp4 for 24 h (96+24 h). Arrowheads (B) mark cells co-expressing lineage markers. (D) Quantification of single-, double- and triple-positive cells for upregulated blood, heart and skeletal muscle markers by immunocytochemistry after 96 h of *in vitro* culture. ***P*<0.01, ****P*<0.001, *****P*<0.0001. *n*=3 independent experiments; six images per experiment. (E,F) Immunofluorescence staining for Gata4 and Pax7 in vehicle- or noggin-treated *ex utero* cultures. Shown are transverse sections of caudal tailbud from *ex utero* embryo cultures. Arrowheads mark endogenous Pax7 expression. Results are representative of three independent experiments. Scale bars: 100 µm.

However, a detailed understanding of the activity of individual Fgfs in tuning the Bmp transcriptional response requires further experimentation.

Aberrant lineage differentiation

A striking observation we made is that the loss of mesoderm progenitor cell identity *in vitro* was accompanied by the upregulation

Development (2017) 144, 2982-2993 doi:10.1242/dev.149955

of distinct gene signatures of muscle, vasculature, bone, heart and blood cell fates. Conversely, mesoderm progenitor cell fate reactivation upon Bmp4 treatment was accompanied by a sharp downregulation of these gene signatures. It is interesting to note that all of the aberrant gene signatures are mesoderm derivatives of the paraxial (muscle and bone/cartilage) and lateral plate splanchnic mesoderm (heart, vasculature and blood). The muscle and bone/cartilage gene signatures are likely to reflect a premature differentiation of mesoderm progenitor cells into somitic derivatives. This is in line with the observation that Bmp signaling needs to be downregulated for proper somite formation (O'Neill and Thorpe, 2013). The dynamic expression pattern of noggin in the tailbud is also consistent with such regulation of progenitor differentiation (Goldman et al., 2000; Ohta et al., 2007). In the mouse, noggin-deficient embryos show an increase in Bmp4 expression associated with posterior somite patterning defects, which can be rescued by lowering *Bmp4* gene dosage (Wijgerde et al., 2005). In zebrafish embryos, Bmp downregulation by specific inhibitors was also required for upregulation of the myogenic program (Reshef et al., 1998; Row and Kimelman, 2009). Hence, the loss of Bmp signaling in mesoderm progenitor cells seems sufficient to trigger part of the differentiation program associated with somite formation.

The distinct upregulation of heart, vasculature and blood gene signatures was more surprising as they are derivatives of another mesoderm compartment, namely the lateral plate mesoderm (Lopez-Sanchez et al., 2001; Psychoyos and Stern, 1996). Hence, Bmp signaling appears to maintain a competence of progenitor cells to derive paraxial mesoderm. In the absence of Bmp signal these cells upregulate other mesoderm markers in an aberrant manner, such that these cells fail to progress towards defined cell fates and instead accumulate in the caudal trunk.

Together, our results point to a crucial role for Bmp signaling in the maintenance of the tailbud mesoderm progenitor cell population in the mouse and clarify the structure of the regulatory network underlying axial elongation.

MATERIALS AND METHODS

Mice and rats

Pax2-GFP BAC transgenic mice were described previously (Bouchard et al., 2005; Pfeffer et al., 2002). Mice were kept in the C57BL/6 genetic background and genotyped using primers listed in Table S17. Appropriate matings were performed and detection of copulatory plugs was designated embryonic day (E) 0.5. Retired breeder rats were used for serum extraction (Takahashi et al., 2014) and acquired from the McGill Comparative Medicine and Animal Resource Centre. All animal experiments were performed in accordance with the ethical guidelines provided by Canadian Council of Animal Care.

FACS analysis and primary tailbud cell cultures

Pax2-GFP embryos were dissected at E9.25-E9.5 and GFP-expressing tailbud cells were separated by FACS analysis as follows. GFP-expressing tailbuds were dissected from the region of the trunk of the embryo caudal to the last somite, followed by trypsinization at 37°C for 15 min to obtain a single-cell suspension. FACS sorting was performed based on granularity and size (SSC, FSC), viability using propidium iodide (PI) (Sigma, 1 µg/ml), and GFP using a FACSAria (BD Biosciences). Sorted PI^-/Pax2-GFP^+ cells were cultured in medium containing DMEM with 10% FBS and 1% penicillin-streptomycin in the presence of mitomycin C-treated (Sigma, 10 µg/ml) mouse embryonic fibroblast (MEF) feeder layers, which were obtained from wild-type C57BL/6 mice. The MEFs were stained with PKH26 Red Fluorescence Cell Linker Dye (Sigma, 2 µM) so that they could be sorted out from the Pax2-GFP^+ tailbud cells after co-culture. Co-cultures were incubated at 37°C in 5% CO_2 for 96 h before treatment with recombinant proteins/growth factors recombinant human (rh) BMP4 (Sigma and USCN, 100 ng/ml), rhFGF8 (Sigma, 100 ng/ml), rhFGF4 (Sigma, 100 ng/ml) and/or recombinant mouse (rm) Wnt3a (Sigma, 100 ng/ml). For cells treated with cycloheximide (Sigma, 1 µg/ml), the treatment was undertaken simultaneously with the growth factor timecourse. Pax2-GFP^+ cells were plated in 50:50 DMEM medium and Matrigel (Sigma) at different cell densities in the absence or presence of rmNoggin (Cedarlane, 100 ng/ml). Cell fluorescence and proliferation were measured every 3 h in IncuCyte-FLR imaging system (Essen BioScience). The average fluorescence intensity of Pax2-GFP^+ tailbud cells at 0 h was set to 100% across different treatments and measured as arbitrary units (A.U.) over time.

High-throughput sequencing

Total RNA was obtained using the RNeasy Micro Kit (Qiagen) following the manufacturer's protocol. Mesoderm progenitor cells from *Pax2-GFP* animals (GFP-expressing or not) were sorted out from PKH26-stained MEFs by FACS as described above. Sequencing libraries were prepared by Genome Quebec Innovation Centre (Montreal, Canada) using the TruSeq Stranded Total RNA Sample Preparation Kit (Illumina, TS-122-2301) by depleting ribosomal and fragmented RNA, synthesizing first- and second-strand cDNA, adenylating the 3′ ends and ligating adaptors, and enriching the adaptor-containing cDNA strands by PCR. The libraries were sequenced using an Illumina HiSeq 2000 sequencer, with 100 nucleotide paired-end reads, generating ~60 million reads per sample. The sequencing reads were trimmed using CutAdapt (Martin, 2011) and mapped to the mouse reference genome (mm10) using STAR aligner (version 2.4.0e) (Dobin et al., 2013), with default parameters, and annotated using the Gencode M2 (version M2, 2013) annotation (Mudge and Harrow, 2015). Htseq-counts [part of the HTSeq (Anders et al., 2015) framework, version 0.5.4p5] was used for expression quantification, and DESeq (Anders and Huber, 2010) for differential expression analysis. Heatmaps and scatter plots were generated using R (version 3.3.1). The Pax2-GFP^{on} gene signature consisted of genes showing significantly higher expression in any Pax2-GFP^{on} cells than in untreated cells at 96 h. The Pax2-GFP^{off} gene signature consisted of genes showing significantly higher expression in any Pax2-GFP^{off} cells than in untreated cells at 0 h.

Quantitative real-time PCR (qRT-PCR)

Total RNA from cultured tailbud cells was extracted using the RNeasy Mini Kit (Qiagen) and reverse transcribed with MMLV (Invitrogen) according to manufacturers' procedures. qRT-PCR was performed using Green-2-Go Mastermix (BioBasic) on a Realplex2 Mastercycler (Eppendorf). Primers are listed in Table S17. All samples were obtained in technical triplicates, and transcript levels were standardized using *B2m*. Biological triplicates were run for both control and treated samples in all the experiments and expression levels were compared using the $2^{-\Delta\Delta CT}$ method (Pfaffl, 2001). One-way ANOVA or unpaired two-tailed Student's *t*-tests were performed using Prism software (GraphPad). Data are presented as mean±s.d.; $P<0.05$ was considered statistically significant.

Embryo cultures

Ex utero live embryo cultures were established as previously described (Gray and Ross, 2011) using E8.75 *Pax2-GFP* embryos. Briefly, embryos were dissected out of the uterus and carefully separated from the decidua, keeping the yolk sac in place, and kept in DMEM medium with 10% FBS and antibiotics. Both vehicle-treated and rmNoggin-treated (Cedarlane,100 ng/ml) embryos were cultured at 37°C and 5% CO_2 in DMEM with 50% rat serum in glass bottles on a roller apparatus (LabQuake).

Immunohistochemistry

Immunofluorescence staining was performed as described previously (Stewart et al., 2013). Tailbud culture cells were plated on glass slides coated with Geltrex (Gibco). E8.75-E9.5 embryos were mounted in Optimal Cutting Temperature (OCT) compound and sectioned to obtain 10-12 µm sections. Antibodies and dilutions used are listed in Table S18.

In situ hybridization

Tissues for *in situ* hybridization were fixed in 4% paraformaldehyde, passed through a sucrose gradient and then embedded in OCT and sectioned at

Development (2017) 144, 2982-2993 doi:10.1242/dev.149955

12 µm. RNA probes for *T* (Herrmann, 1991) and *Bmp4* (Wall and Hogan, 1995) were synthesized using T7 or SP6 RNA polymerase following the manufacturer's specifications (Roche) for *in situ* hybridization.

Microscopy and image analysis

Bright-field whole-mount images were acquired with a Stemi 2000-C microscope (Zeiss) and sections were imaged using an Axioplan 2 microscope (Zeiss). Immunofluorescence images were acquired using either an Observer.Z1 (Zeiss) or an LSM3, LSM710 or LSM800 confocal microscope (Zeiss) at the Advanced BioImaging Facility of McGill University. Quantification and image analysis were performed using Zen (Zeiss) and Fiji (ImageJ) software.

Acknowledgements

We are grateful to members of the M.B. laboratory and Dr Yojiro Yamanaka for critical reading of the manuscript. We thank the McGill Advanced BioImaging Facility (ABIF) for technical support with confocal microscopy, and the Flow Cytometry Platform of the McGill University Life Sciences Complex for Cell Sorting.

Competing interests

The authors declare no competing or financial interests.

Author contributions

Conceptualization: R.S., M.B.; Methodology: R.S., M.E.R.S., M.T.; Software: M.E.R.S., E.B., J.M.; Validation: R.S., M.E.R.S., E.B.; Formal analysis: R.S., M.T., M.B.; Investigation: R.S., M.B.; Resources: J.M., M.B.; Data curation: R.S., M.E.R.S., E.B.; Writing - original draft: R.S., M.B.; Writing - review & editing: R.S., M.E.R.S., M.T., M.B.; Visualization: R.S., M.E.R.S.; Supervision: M.B.; Project administration: M.B.; Funding acquisition: M.B.

Funding

This work was supported by a grant from the Canadian Institutes of Health Research (CIHR) (MOP-130431) to M.B. M.B. holds a Senior Research Scholar Award from the Fonds de la Recherche du Québec-Santé (FRQS). R.S. was supported by a Rolande and Marcel Gosselin Graduate Studentship from the Faculty of Medicine, McGill University. M.E.R.S. was supported by a Graduate Studentship from Prostate Cancer Canada, and a Lloyd-Carr Harris Graduate Studentship from McGill University. J.M. was supported by CIHR, and E.B. was supported by FORGE Canada Consortium through Care For Rare Project. M.T. was supported by a Dr Gerald B. Price Fellowship (Cancer Research Society), McGill Integrated Cancer Research Training Program (MICRTP) of McGill University and FRQS postdoctoral fellowships.

Data availability

The RNA-seq data have been deposited at Gene Expression Omnibus with accession number GSE101810.

Supplementary information

Supplementary information available online at
http://dev.biologists.org/lookup/doi/10.1242/dev.149955.supplemental

References

Anders, S. and Huber, W. (2010). Differential expression analysis for sequence count data. *Genome Biol.* **11**, R106.

Anders, S., Pyl, P. T. and Huber, W. (2015). HTSeq–a Python framework to work with high-throughput sequencing data. *Bioinformatics* **31**, 166-169.

Aulehla, A. and Pourquie, O. (2010). Signaling gradients during paraxial mesoderm development. *Cold Spring Harb. Perspect. Biol.* **2**, a000869.

Beck, C. W., Whitman, M. and Slack, J. M. W. (2001). The role of BMP signaling in outgrowth and patterning of the Xenopus tail bud. *Dev. Biol.* **238**, 303-314.

Bénazéraf, B., Francois, P., Baker, R. E., Denans, N., Little, C. D. and Pourquié, O. (2010). A random cell motility gradient downstream of FGF controls elongation of an amniote embryo. *Nature* **466**, 248-252.

Bouchard, M., Souabni, A., Mandler, M., Neubuser, A. and Busslinger, M. (2002). Nephric lineage specification by Pax2 and Pax8. *Genes Dev.* **16**, 2958-2970.

Bouchard, M., Grote, D., Craven, S. E., Sun, Q., Steinlein, P. and Busslinger, M. (2005). Identification of Pax2-regulated genes by expression profiling of the mid-hindbrain organizer region. *Development* **132**, 2633-2643.

Boulet, A. M. and Capecchi, M. R. (2012). Signaling by FGF4 and FGF8 is required for axial elongation of the mouse embryo. *Dev. Biol.* **371**, 235-245.

Deschamps, J. and van Nes, J. (2005). Developmental regulation of the Hox genes during axial morphogenesis in the mouse. *Development* **132**, 2931-2942.

Diez del Corral, R., Olivera-Martinez, I., Goriely, A., Gale, E., Maden, M. and Storey, K. (2003). Opposing FGF and retinoid pathways control ventral neural pattern, neuronal differentiation, and segmentation during body axis extension. *Neuron* **40**, 65-79.

Dobin, A., Davis, C. A., Schlesinger, F., Drenkow, J., Zaleski, C., Jha, S., Batut, P., Chaisson, M. and Gingeras, T. R. (2013). STAR: ultrafast universal RNA-seq aligner. *Bioinformatics* **29**, 15-21.

Galceran, J., Hsu, S.-C. and Grosschedl, R. (2001). Rescue of a Wnt mutation by an activated form of LEF-1: regulation of maintenance but not initiation of Brachyury expression. *Proc. Natl. Acad. Sci. USA* **98**, 8668-8673.

Goldman, D. C., Martin, G. R. and Tam, P. P. (2000). Fate and function of the ventral ectodermal ridge during mouse tail development. *Development* **127**, 2113-2123.

Gray, J. and Ross, M. E. (2011). Neural tube closure in mouse whole embryo culture. *J. Vis. Exp.* **56**, pii: 3132.

Herrmann, B. G. (1991). Expression pattern of the Brachyury gene in whole-mount TWis/TWis mutant embryos. *Development* **113**, 913-917.

Hubaud, A. and Pourquié, O. (2014). Signalling dynamics in vertebrate segmentation. *Nat. Rev. Mol. Cell Biol.* **15**, 709-721.

Inman, K. E. and Downs, K. M. (2006). Localization of Brachyury (T) in embryonic and extraembryonic tissues during mouse gastrulation. *Gene Expr. Patterns* **6**, 783-793.

Kuschert, S., Rowitch, D. H., Haenig, B., McMahon, A. P. and Kispert, A. (2001). Characterization of Pax-2 regulatory sequences that direct transgene expression in the Wolffian duct and its derivatives. *Dev. Biol.* **229**, 128-140.

Lopez-Sanchez, C., Garcia-Martinez, V. and Schoenwolf, G. C. (2001). Localization of cells of the prospective neural plate, heart and somites within the primitive streak and epiblast of avian embryos at intermediate primitive-streak stages. *Cells Tissues Organs* **169**, 334-346.

Martin, M. (2011). Cutadapt removes adapter sequences from high-throughput sequencing reads. *EMBnet.Journal* **17**, 10-12

McMahon, J. A., Takada, S., Zimmerman, L. B., Fan, C.-M., Harland, R. M. and McMahon, A. P. (1998). Noggin-mediated antagonism of BMP signaling is required for growth and patterning of the neural tube and somite. *Genes Dev.* **12**, 1438-1452.

Messenger, N. J., Kabitschke, C., Andrews, R., Grimmer, D., Nunez Miguel, R., Blundell, T. L., Smith, J. C. and Wardle, F. C. (2005). Functional specificity of the Xenopus T-domain protein Brachyury is conferred by its ability to interact with Smad1. *Dev. Cell* **8**, 599-610.

Mudge, J. M. and Harrow, J. (2015). Creating reference gene annotation for the mouse C57BL6/J genome assembly. *Mamm. Genome* **26**, 366-378.

Naiche, L. A., Holder, N. and Lewandoski, M. (2011). FGF4 and FGF8 comprise the wavefront activity that controls somitogenesis. *Proc. Natl. Acad. Sci. USA* **108**, 4018-4023.

Neijts, R., Simmini, S., Giuliani, F., van Rooijen, C. and Deschamps, J. (2014). Region-specific regulation of posterior axial elongation during vertebrate embryogenesis. *Dev. Dyn.* **243**, 88-98.

Ohta, S., Suzuki, K., Tachibana, K., Tanaka, H. and Yamada, G. (2007). Cessation of gastrulation is mediated by suppression of epithelial-mesenchymal transition at the ventral ectodermal ridge. *Development* **134**, 4315-4324.

O'Neill, K. and Thorpe, C. (2013). BMP signaling and spadetail regulate exit of muscle precursors from the zebrafish tailbud. *Dev. Biol.* **375**, 117-127.

Pfaffl, M. W. (2001). A new mathematical model for relative quantification in real-time RT-PCR. *Nucleic Acids Res.* **29**, e45.

Pfeffer, P. L., Payer, B., Reim, G., di Magliano, M. P. and Busslinger, M. (2002). The activation and maintenance of Pax2 expression at the mid-hindbrain boundary is controlled by separate enhancers. *Development* **129**, 307-318.

Psychoyos, D. and Stern, C. D. (1996). Fates and migratory routes of primitive streak cells in the chick embryo. *Development* **122**, 1523-1534.

Pyati, U. J., Webb, A. E. and Kimelman, D. (2005). Transgenic zebrafish reveal stage-specific roles for Bmp signaling in ventral and posterior mesoderm development. *Development* **132**, 2333-2343.

Reshef, R., Maroto, M. and Lassar, A. B. (1998). Regulation of dorsal somitic cell fates: BMPs and Noggin control the timing and pattern of myogenic regulator expression. *Genes Dev.* **12**, 290-303.

Row, R. H. and Kimelman, D. (2009). Bmp inhibition is necessary for post-gastrulation patterning and morphogenesis of the zebrafish tailbud. *Dev. Biol.* **329**, 55-63.

Stewart, K., Uetani, N., Hendriks, W., Tremblay, M. L. and Bouchard, M. (2013). Inactivation of LAR family phosphatase genes Ptprs and Ptprf causes craniofacial malformations resembling Pierre-Robin sequence. *Development* **140**, 3413-3422.

Stickney, H. L., Imai, Y., Draper, B., Moens, C. and Talbot, W. S. (2007). Zebrafish bmp4 functions during late gastrulation to specify ventroposterior cell fates. *Dev. Biol.* **310**, 71-84.

Takahashi, M., Makino, S., Kikkawa, T. and Osumi, N. (2014). Preparation of rat serum suitable for mammalian whole embryo culture. *J. Vis. Exp.* **90**, e51969.

Development (2017) 144, 2982-2993 doi:10.1242/dev.149955

Wahl, M. B., Deng, C., Lewandoski, M. and Pourquie, O. (2007). FGF signaling acts upstream of the NOTCH and WNT signaling pathways to control segmentation clock oscillations in mouse somitogenesis. *Development* **134**, 4033-4041.

Wall, N. A. and Hogan, B. L. M. (1995). Expression of bone morphogenetic protein-4 (BMP-4), bone morphogenetic protein-7 (BMP-7), fibroblast growth factor-8 (FGF-8) and sonic hedgehog (SHH) during branchial arch development in the chick. *Mech. Dev.* **53**, 383-392.

Welsh, I. C. and O'Brien, T. P. (2000). Loss of late primitive streak mesoderm and interruption of left-right morphogenesis in the Ednrb(s-1Acrg) mutant mouse. *Dev. Biol.* **225**, 151-168.

Wijgerde, M., Karp, S., McMahon, J. and McMahon, A. P. (2005). Noggin antagonism of BMP4 signaling controls development of the axial skeleton in the mouse. *Dev. Biol.* **286**, 149-157.

Wilson, V., Olivera-Martinez, I. and Storey, K. G. (2009). Stem cells, signals and vertebrate body axis extension. *Development* **136**, 1591-1604.

Winnier, G., Blessing, M., Labosky, P. A. and Hogan, B. L. (1995). Bone morphogenetic protein-4 is required for mesoderm formation and patterning in the mouse. *Genes Dev.* **9**, 2105-2116.

Yamaguchi, T. P., Takada, S., Yoshikawa, Y., Wu, N. and McMahon, A. P. (1999). T (Brachyury) is a direct target of Wnt3a during paraxial mesoderm specification. *Genes Dev.* **13**, 3185-3190.

Yang, X., Dormann, D., Münsterberg, A. E. and Weijer, C. J. (2002). Cell movement patterns during gastrulation in the chick are controlled by positive and negative chemotaxis mediated by FGF4 and FGF8. *Dev. Cell* **3**, 425-437.

Yoon, J. K., Moon, R. T. and Wold, B. (2000). The bHLH class protein pMesogenin1 can specify paraxial mesoderm phenotypes. *Dev. Biol.* **222**, 376-391.

Supplementary Figures and Tables

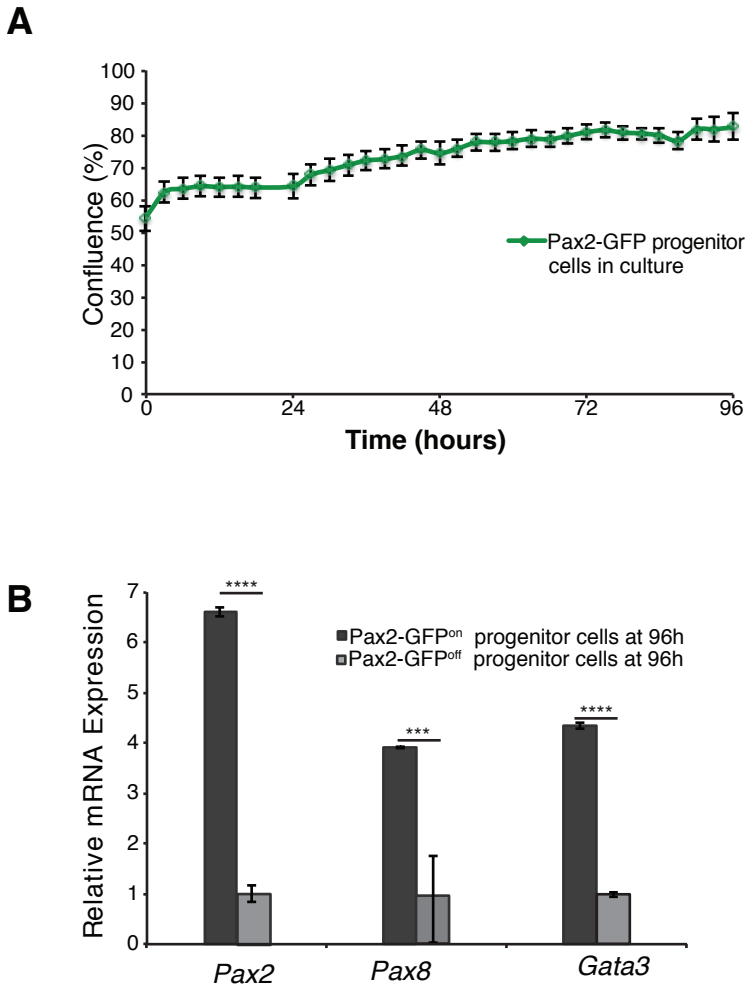

Supplementary Figure 1

A) Measurement of Pax2-GFP^{+ve} tailbud progenitor cell confluence over 96h in culture. Loss of fluorescence is not accompanied by a loss Pax2-GFP tailbud progenitors over 96h. B) qRT-PCR of renal markers in sorted Pax2-GFP^{on} cells which remain after 96h of co-culture with MEFs. mRNA levels were normalized to B2m and to Pax2-GFP^{off} cells at 96h (Mean +/- SD, n=3). Student's t-test was used to determine statistical differences.

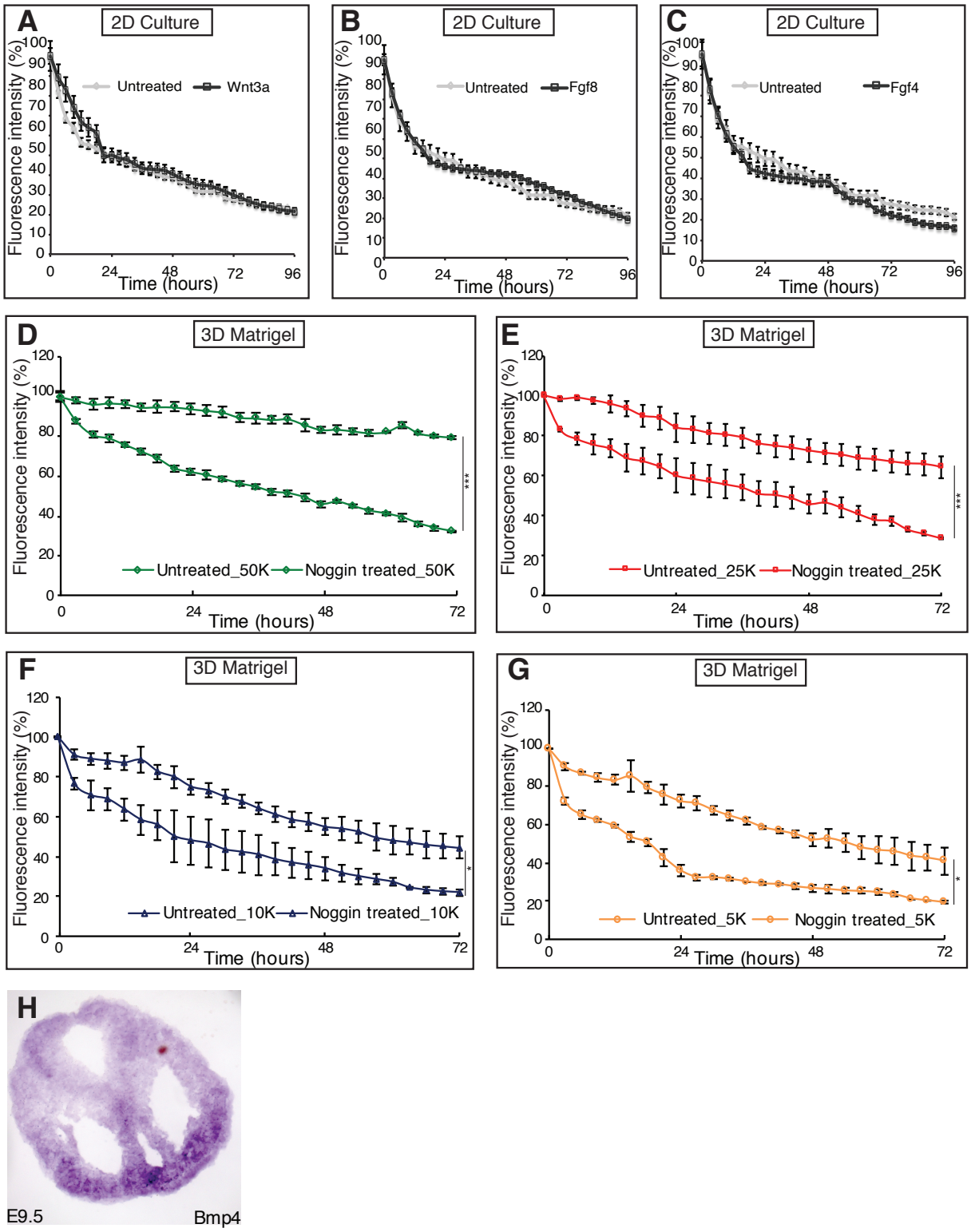

Supplementary Figure 2

Measurement and quantification of Pax2-GFP expression over 96h in culture. A-C) Fluorescence intensity (%) of Pax2-GFP tailbud mesoderm progenitors treated with Wnt3A (A) Fgf8 (B) or Fgf4 (C). (Mean +/- SD, n=3). Mesoderm progenitors were co-cultured with MEFs. (D-G) Pax2-GFP^{+ve} tailbud mesoderm progenitor cells were plated in 3D matrigel cultures and GFP fluorescence was measured over 72 hours when treated with Bmp inhibitor Noggin at different densities. D) 50,000 cells (50K) E) 25,000 cells (25K) F) 10,000 cells (10K) G) 5,000 cells (5K). The statistical differences were calculated using Student's t-test. H) In situ hybridization of *Bmp4* shows the expression domain in the ventral mesoderm region of transversal sections of E9.5 embryo tailbud (20X).

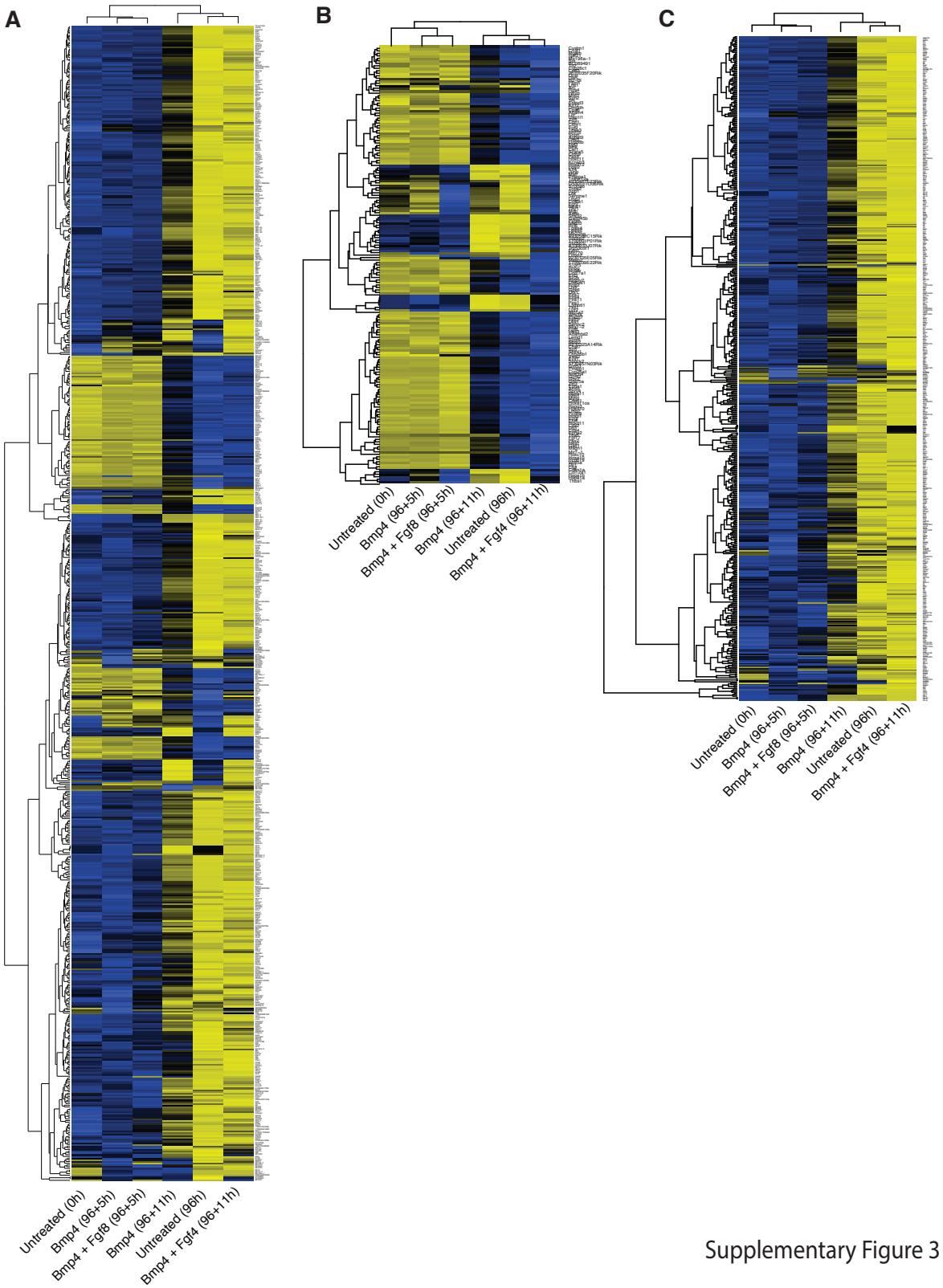

Supplementary Figure 3

Supplementary Figure 3

A) Heatmap of RNA read counts of differentially regulated genes identified by pairwise comparisons performed between conditions, which were used to identify gene signatures. B) Heatmap of genes upregulated in Pax2-GFP^{on} cells (Pax2-GFP^{on} signature). C) Heatmap of genes upregulated in Pax2-GFP^{off} cells (Pax2-GFP^{off} signature).

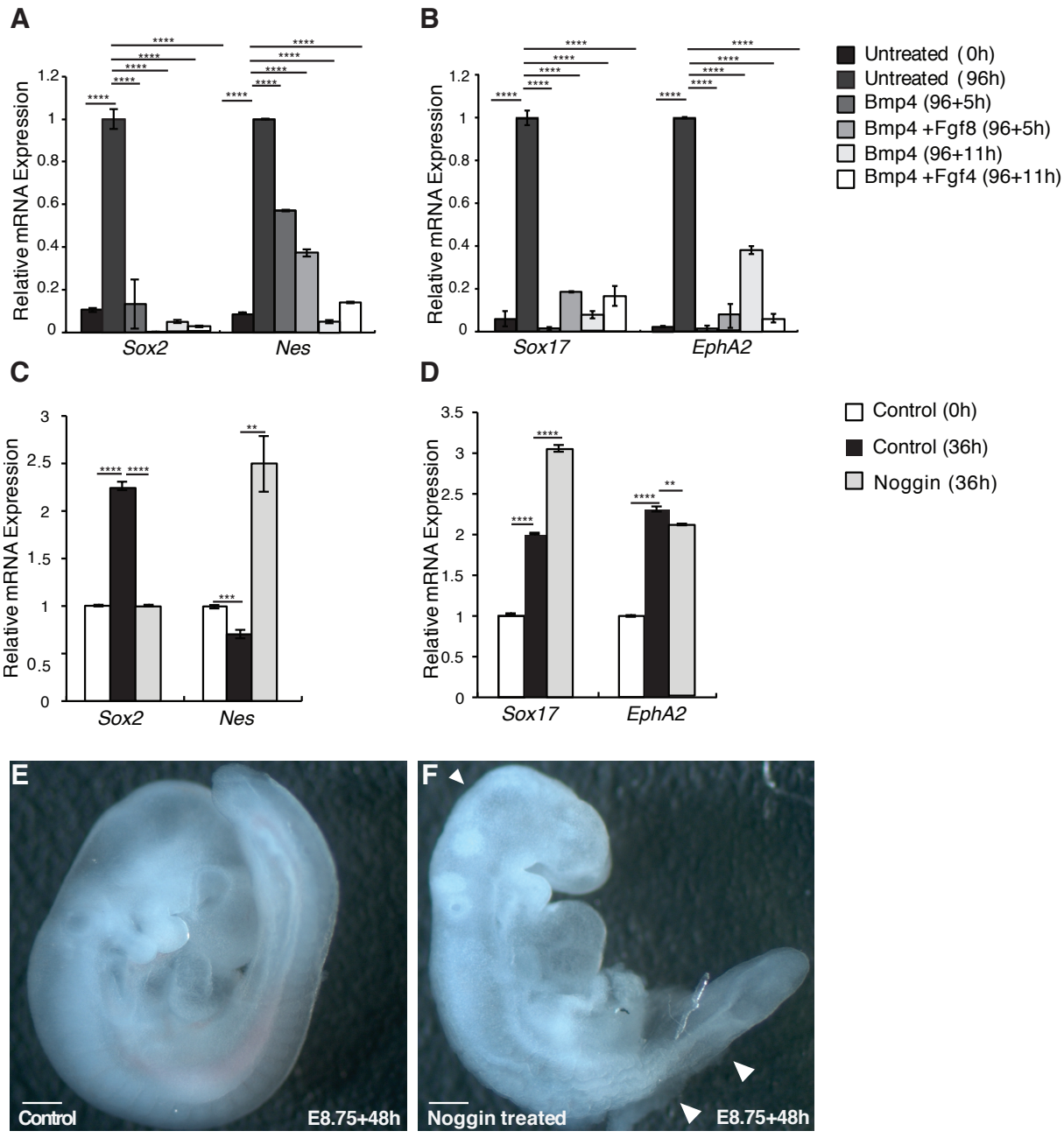

Supplementary Figure 4

A-B) qRT-PCR of neural and hindgut lineage markers from cells untreated at 0h and 96h or treated with Bmp4 alone, with Fgf8 or with Fgf4 at 96h post initial plating for 5h or 11h respectively. Cells used for RNA extraction were sorted out from MEFs. mRNA levels are normalized to *B2m* and to untreated cells at 96h. (Mean +/- SD, n=3). One-way Anova was used to calculate statistical significance and all samples were compared to untreated at 96h.

C-D) qRT-PCR of neural and hindgut marker genes *Sox2, Nestin, Sox17 and EphA2* in *ex utero* cultured embryos treated or not with Noggin. mRNA levels were normalized to *B2m*. One-way Anova was used to determine statistical differences and all samples were compared to control at 36h. (Mean +/- SD, n=3)

E-F) Embryos dissected at E8.75 and cultured *ex utero* for 48 hours in the presence or absence of recombinant Noggin show abnormalities in somites, neural tube and tailbud development (arrowhead points to defects of somites, neural tube and tailbud); Scale bars-1000μm, n=3

Tables S1-S12. Pairwise comparisons of mesoderm progenitors in all conditions distinguishes a Pax2-GFPon (green) and a Pax2-GFPoff (black) signature

Click here to Download Tables S1 - S12

Tables S13-S16. Genes differentially regulated in the Pax2-GFPon (Table S13) or Pax2-GFPoff (Table S14) signatures, including those in the Pax2-GFPon signature identified as presomitic mesoderm associated (Table S15) and those in the Pax2-GFPoff signature distinctly associated with muscle, heart, blood, bone and endothelial cell signatures (Table S16).

Click here to Download Tables S13 - S16

Supplementary Table S17

The primer sequences used for genotyping and qPCR analyses

Primers	Forward Primer	Reverse Primer
Pax2_geno	ACTGGTGTGAGAGGCGGGTTCTT	AAACAGGCAGAGTGGCTGAGTAT
Pax2GFP_geno	GCTGGCGAAAGGGGGATGTGCTG	AAACAGGCAGAGTGGCTGAGTAT
mPax2_qPCR	CGGTGGCACTGGGACGCAAGG	GAGGAAGCACAGGAGGGAAAG
mPax8_qPCR	GGGCTCTACCTACTCTATCAA	GGACCACTGCTGCTGCTCTGT
mGata3_qPCR	ACAGAAGGCAGGGAGTGTGTGAAC	ATGGTAGAGTCCGCAGGCATTG
mMesogenin1_qPCR	CCAGCTCCTTCTCTGGAGTC	AGCCAACATGCTGTAATCCA
mCdx4_qPCR	TTCTTCACCACTCCATCTGC	GAAGGATGCTTCCGTTTCTC
mBrachyury_qPCR	GCGGGAAAGAGCCTGCAGTA	TTCCCCGTTCACGTACTTCC
mNkx1-2_qPCR	TTCTGGACCTCATTCTTCCC	CTGGGAACCCTTATTAGCCA
mMyh6_qPCR	GAGGACCAGGCCAATGAGTA	GCTGGGTGTAGGAGAGCTTG
mCol3a1_qPCR	GGAGCCCCTGGACTAATAGG	ATCCATCTTTGCCATCTTCG
mGata6_qPCR	GAGCTGGTGCTACCAAGAGG	TGCAAAAGCCCATCTCTTCT
mActa2_qPCR	TGTGCTGGACTCTGGAGATG	GAAGGAATAGCCACGCTCAG
mHba-x_qPCR	CTGTCTGCTGGTCACAATGG	GGGAGGAGAGGGATCATAGC
mHbb-y_qPCR	CTTGGGTAATGTGCTGGTGA	GTGCAGAAAGGAGGCATAGC
mCdh5_qPCR	GTTGCCACATCTCAGGGAAT	CCTTCCTCCAGCTGTCACTC
mPax1_qPCR	CAGCAAACCTCGAGTTACCA	GGGCACGTTGTACTTGTCAC
mSox2_qPCR	AAGGGTTCTTGCTGGGTTTT	AGACCACGAAAACGGTCTTG
mNestin_qPCR	GGAACCCAGAGACTGTGGAA	CACATCCTCCCACCTCTGTT
mSox17_qPCR	GCCCTCATGAACTTGCTCTC	TACAGCGAGCCTCAGAGTGA
mEphA2_qpcr	ACTATGGCGGCTGTATGTCC	TCTAGCGCTCCATTCTCCAT

Supplementary Table S18

Antibodies used for immunocytochemistry and immunofluorescence staining

Antibody	Source	Dilution
GFP (Rabbit)	Invitrogen, a6455	1:200
Ter119 (Biotin)	Stemcell Technologies, 60033AD	1:100
Gata4 (Mouse)	Santa Cruz, sc-25310	1:50
Pax7 (Chicken)	Supernatant, DHSB	1:10